

AGV CORRIDOR NAVIGATION BASED ON DATA FUSION

CARLOS SORIA, RICARDO CARELLI

*Instituto de Automática – Universidad Nacional de San Juan
Av. San Martín Oeste, 5400 San Juan, Argentina
E-mails: csoria@inaut.unsj.edu.ar, rcarelli@inaut.unsj.edu.ar*

EDUARDO FREIRE

*Núcleo de Engenharia Elétrica – Centro de Ciências Exatas e Tecnologia – Universidade Federal de Sergipe
Av. Marechal Rondon S/N, Jardim Rosa Elze, São Cristovão/SE, Brasil
E-mail: efreire@ufs.br*

Abstract— This work presents a control strategy for mobile robots navigating in corridors, using the data fusion from ultrasonic and vision sensors. The controller generates angular velocity commands to keep the robot navigating along the corridor. The fusion of both data signals is done through a Decentralized Information Filter. Experiments on a laboratory robot are presented to show the feasibility and performance of the proposed control system.

Keywords— Sensor Fusion, Mobile Robot, Artificial Vision, H_∞ control.

1 Introduction

A main characteristic of Autonomous Navigation is its capability of capturing environment information through external sensors, such as vision, distance or proximity sensors. Although distance sensors (e.g., ultrasound and laser types), which allow to detect obstacles and measure distances to walls and obstacles near the robot, are the most usual sensors, at present vision sensors are increasingly used because they render a greater amount of information from visual images.

When autonomous mobile robots navigate within indoor environments (e.g., public buildings or industrial facilities) they should be endowed the capability to move along corridors, to turn at corners and to come into rooms. As regards motion along corridors, some control algorithms have been proposed in various works. In (Bemporad, *et al.*, 1997), a globally stable control algorithm for wall-following based on incremental encoders and one sonar sensor is developed. In (Vasallo *et al.*, 1998), image processing is used to detect perspective lines and to guide the robot following the corridor centerline. This work assumes an elementary control law and does not prove control stability. In (Yang, Tsai, 1999), ceiling perspective lines are employed for robot guidance, but it also lacks a demonstration on system stability. Other authors have proposed to use the technique of optical flow for corridor centerline guidance. Some approaches incorporate two video cameras on the robot sides, and the optical flow is computed to compare the apparent velocity of image patterns from both cameras (Santos-Victor *et al.*, 1995). In (Dev *et al.*, 1997), a camera is used to guide a robot along a corridor centerline or to follow a wall. In (Servic *et al.*, 2001) perspective lines are used to find the absolute orientation within a corridor. In (Carelli *et al.*, 2002) the authors have

proposed the fusion of the outputs of two vision-based controllers using a Kalman Filter in order to guide the robot along the centerline of a corridor. One of the controllers is based on optical flow, and the other is based on the perspective lines of the corridor.

The objective of the tracking control is to assure that the output of a system track a given time varying reference. For example, the tracking controller in a mobile robot is required to drive the robot states to the desired states given as time functions.

This work is based on the robot kinematics model to design the controller for tracking a line reference (the corridor's center). The linear matrix inequalities (LMI) (Boyd *et al.*, 1994), due to their highly-efficient solutions, have attracted the attention of the control area, and it has become an important method in the analysis and design of controllers. The LMIs can be solved efficiently by interior-point optimization algorithms (Nesterov *et al.*, 1996), especially Matlab LMI Control Toolbox (Gahinet *et al.*, 1994). Using the linearized kinematics model of the mobile robot at the equilibrium point, a tracking control based on H_∞ via LMI is designed. H_∞ control theory has become a standard design method in the last 15 years, which shows the usefulness of H_∞ norm performance index (Zhou *et al.*, 1997), (Goddard *et al.*, 1998), (Mattei, 2000), (Saeki and Aimoto, 2000).

In the present work, we find the perspective lines of the walls meeting the floor and fuse this information with the data obtained from ultrasonic sensors to estimate the robot position with respect to the centerline of the corridor. Based on this information, a controller is used to generate the angular velocity command for the robot. The linear velocity of the robot may either be kept constant. The work also includes experimental results on a Pioneer 2 DX laboratory robot navigating through the corridors at the Institute of

Automatics, National University of San Juan, Argentina.

This paper is organized as follows. In section 2, the mobile robot kinematics model and the camera model is presented. In section 3, the data fusion of the variables obtained by the sensorial information. The design of the controllers is shown in section 4, and the experimental results are presented in section 5.

2 Robot and Camera Models

2.1 Robot Model

Fig. 1 represents the coordinate systems associated to the robot and the environment: a world system [W], a system [R] fixed to the robot and a system [C] fixed to the vision camera. Considering Fig. 1, the kinematics model of a unicycle type robot can be expressed as (Dixon *et al.*, 2001),

$$\begin{cases} \dot{x} = v \sin \theta \\ \dot{y} = v \cos \theta \\ \omega = \dot{\theta} \end{cases} \quad (1)$$

where ω is the angular velocity and v the linear velocity of the robot, $x \equiv {}^W x_{or}$, $y \equiv {}^W y_{or}$.

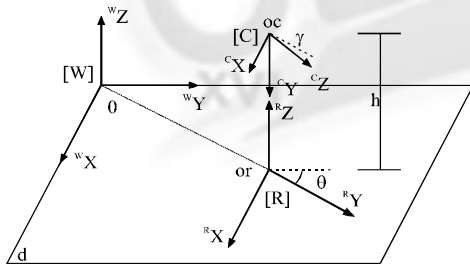


Fig. 1. Coordinate systems.

2.2 Camera Model

A pinhole model for the camera is considered. The following relationship can be immediately obtained from Fig. 2,

$$r = \alpha \lambda \frac{p}{c p_z} \quad (2)$$

where r is the projection of a point p on the image plane, λ is the focal length of the camera and α is a scale factor.

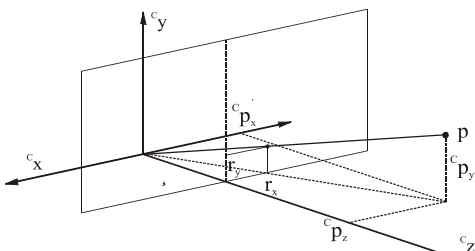


Fig. 2. Perspective projection camera model.

2.3 Model for the perspective lines

The position and orientation of the robot can be obtained from the projection of the perspective lines in the corridor on the image plane. The parallel lines resulting from the intersection of corridor walls and floor are projected onto the image plane as two lines intersecting at the so-called vanishing point.

A point p in the global frame [W] can be expressed in the camera frame [C] as, ${}^C p = {}^C R_W ({}^W p - p_{oc}) - {}^C R_R P_{oc}$

where

$${}^C R_R = \begin{bmatrix} 1 & 0 & 0 \\ 0 & -\sin(\gamma) & -\cos(\gamma) \\ 0 & \cos(\gamma) & -\sin(\gamma) \end{bmatrix},$$

and

$${}^C R_W = \begin{bmatrix} \cos(\theta) & -\sin(\theta) & 0 \\ -\sin(\theta)\sin(\gamma) & -\cos(\theta)\sin(\gamma) & -\cos(\gamma) \\ \sin(\theta)\cos(\gamma) & \cos(\theta)\cos(\gamma) & -\sin(\gamma) \end{bmatrix}.$$

with γ the camera tilt angle and θ the robot heading.

Considering the component-wise expressions for the pinhole camera model (2),

$$r_x = \alpha_x \lambda \frac{{}^C p_x}{{}^C p_z}, \quad r_y = \alpha_y \lambda \frac{{}^C p_y}{{}^C p_z} \quad (4)$$

any point in the global coordinate system is represented in the image plane as a projection point with coordinates

$$r_x = \alpha_x \lambda \frac{\cos(\theta)({}^W p_x - {}^W p_{xor}) - \sin(\theta)\sin(\gamma)({}^W p_x - {}^W p_{xor}) + \cos(\theta)\sin(\gamma)({}^W p_y - {}^W p_{yor}) - \sin(\gamma)h}{\sin(\theta)\cos(\gamma)({}^W p_x - {}^W p_{xor}) + \cos(\theta)\sin(\gamma)({}^W p_y - {}^W p_{yor}) - \sin(\gamma)h} \quad (5)$$

$$r_y = \alpha_y \lambda \frac{-\sin(\theta)\sin(\gamma)({}^W p_x - {}^W p_{xor}) - \cos(\theta)\sin(\gamma)({}^W p_y - {}^W p_{yor}) - \cos(\gamma)h}{\sin(\theta)\cos(\gamma)({}^W p_x - {}^W p_{xor}) + \cos(\theta)\sin(\gamma)({}^W p_y - {}^W p_{yor}) - \sin(\gamma)h} \quad (6)$$

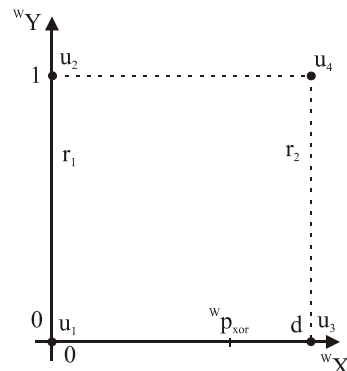


Fig. 3. Guide lines in the corridor.

Now consider the points $u_1 = [0 \ 0 \ 0]^T$, $u_2 = [0 \ 1 \ 0]^T$, $u_3 = [d \ 0 \ 0]^T$, $u_4 = [d \ 1 \ 0]^T$ that define

the intersection lines $r_1 = (u_1, u_2)$ and $r_2 = (u_3, u_4)$ between corridor walls and floor, as illustrated in Fig. 3. Based on (5) and (6), the following relationships are obtained for the slope of the perspective lines, the vanishing point coordinates and the intersection of both lines with the horizontal axis in the image plane, Fig.5 .

$$m_1 = \frac{\alpha_y}{\alpha_x} \frac{h \cos(\theta)}{(\cos(\gamma))^W p_{xor} + \sin(\theta) \sin(\gamma) h} \quad (7)$$

$$m_2 = \frac{\alpha_y}{\alpha_x} \frac{h \cos(\theta)}{(\cos(\gamma))^W p_{xor} - d + \sin(\theta) \sin(\gamma) h} \quad (8)$$

$$x_v = -\frac{\alpha_x \lambda \tan(\theta)}{\cos(\gamma)} \quad (9)$$

$$y_v = \alpha_y \lambda \tan(\gamma) \quad (10)$$

$$\frac{b_1}{m_1} = \frac{\alpha_x \lambda (\sin(\theta) \cos(\gamma) h - {}^W p_{xor} \sin(\gamma))}{h \cos(\theta)} \quad (11)$$

$$\frac{b_2}{m_2} = \alpha_x \lambda \frac{(d - {}^W p_{xor}) \sin(\gamma) + h \sin(\theta) \cos(\gamma)}{h \cos(\theta)} \quad (12)$$

3 Data Fusion

3.1 Data from Ultrasonic Sensors

The controller based on the position of the robot with respect to the centerline of the corridor is required to be back fed with the values of states $\tilde{x}(t)$ and $\theta(t)$ at each instant. These values can also be obtained from sonar measurements. Fig. 4 shows a typical situation where lateral sonar sensors $S_0, S_{15}, S_7,$ and S_8 are used and d is the distance between the lateral sonar sensors. For this case, the following equations allow calculating the state variables,

$$dleft = \frac{y_{s0} + y_{s15}}{2}; \quad dright = \frac{y_{s7} + y_{s8}}{2} \quad (13)$$

$$diff = \frac{(y_{s0} - y_{s15}) + (y_{s7} - y_{s8})}{2} \quad (14)$$

$$\theta = \sin^{-1}\left(\frac{diff}{d}\right); \quad \tilde{x} = \frac{(dright - dleft)}{2} \quad (15)$$

Sonar measurements may deteriorate or be impossible to obtain under certain circumstances, like - for example- when the robot is traveling by an open door in the corridor, or when the robot has a significant angle of deviation from the corridor axis. The latter condition originates from the fact that a sonar sensor collects useful data only when its direction orthogonal to the reflecting surface lies within the beam width of the receiver, thus allowing for wall detection only for a restricted heading range (Bemporad *et al.*, 1997). The range for this angle is approximately $\varphi = 17^\circ$ for the electrostatic sensors in the robot used in the experiments. On this account, it is important to consider other measurements as well, such as the odometric data provided by the robot. The fusion of these data using optimal filters produces optimal

estimations of the robot states, thus minimizing the uncertainty in the sensor measurements. Some authors, e.g. (Sasiadek *et al.*, 2000), have fused the odometric and sonar data. In this work we fuse the sonar data with the vision data described in the next section. Here, we propose to fuse the sonar measurements \tilde{x}_1, θ_1 and the vision measurements \tilde{x}_2, θ_2 , by using a distributed information filter, DIF.

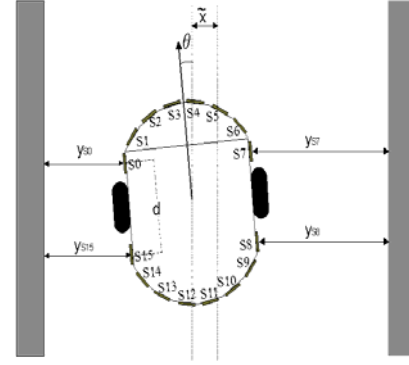


Fig. 4. Calculation of state variables from distance measurements.

3.2 Data from Vision Sensor

It is important to express the control objective of navigating along the corridor centerline in terms of the image features from perspective lines. The robot is following the centerline of the corridor when the slope of both perspective lines become equal; that is, when x_v -the vanishing point- and δ_x -the middle point between the intersection of both perspective lines with the horizontal axis- are equal to zero, Fig. 5. In the workspace, orientation robot error θ and position robot error relative to the center of the corridor $\tilde{x} = {}^W p_{xor} - d/2$ are defined. These errors can be expressed in terms of the image features x_v and δ_x . Equation (9) can be written as,

$$x_v = K_1 \tan(\theta), \quad K_1 = -\frac{\alpha_x \lambda}{\cos(\gamma)}$$

from which,

$$\theta = \arctan\left(\frac{x_v}{K_1}\right) \quad (16)$$

Besides,

$$\delta_x = -\frac{1}{2} \left(\frac{b_1}{m_1} + \frac{b_2}{m_2} \right)$$

By substituting (11) and (12),

$$\delta_x = -\alpha_x \lambda \frac{h \sin(\theta) \cos(\gamma) - \sin(\gamma) ({}^W p_{xor} - d/2)}{h \cos(\theta)}$$

and recalling that $\tilde{x} = {}^W p_{xor} - d/2$, \tilde{x} can be explicitly expressed as

$$\tilde{x} = \frac{\cos(\theta)}{K_2} (\delta_x - K_3 \tan(\theta)) \quad (17)$$

where $K_2 = \alpha_x \lambda \frac{\sin(\gamma)}{h}$, $K_3 = -\alpha_x \lambda \cos(\gamma)$.

Eqs. (16) and (17) render the orientation and position errors as a function of x_v and δ_x .

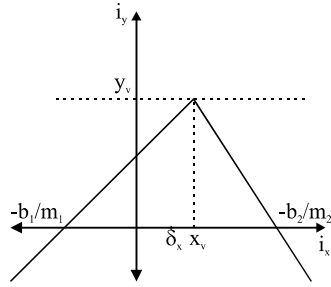


Fig. 5. Perspective lines.

3.3 Decentralized Information Filter

The state variables $\tilde{x}(t)$ and $\theta(t)$ obtained using the data from the ultrasonic and vision sensors are fused using a decentralized information filter (DIF) as presented in Fig. 6. Two local filters and a global filter compose this filter. Each local filter processes the data from one kind of sensor (ultrasonic or vision) and calculates its information vector (y) and information matrix (Y), (see Fig. 6), which could be used to find its local estimated state variables. The information vector and information matrix calculated by each local filter is then passed to the global filter, which in turn calculates the optimal estimated state variables. The information matrix is the inverse of the covariance matrix P of the Kalman filter and the vector of information is obtained by multiplying the information matrix by the state vector. More information about this fusion by DIF is given in (Freire, 2004).

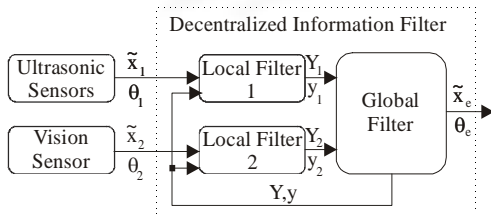


Fig 6. Decentralized Information Filter.

4 Controller Design

It is assumed that the reference trajectory is generated by the following virtual robot.

$$\begin{aligned}\dot{x}_r &= v_r \cos \theta_r \\ \dot{y}_r &= v_r \sin \theta_r \\ \dot{\theta}_r &= \omega_r\end{aligned}\quad (18)$$

where (x_r, y_r, θ_r) are the position and the orientation of the virtual robot; v_r and ω_r are the linear and angular velocities of the virtual robot, respectively. Using the robot coordinates (i.e. the moving coordinate's systems x - y , of Fig. 7), the error coordinates (Kanayama *et al.*, 1990) can be defined as:

$$\begin{bmatrix} x_e \\ y_e \\ \theta_e \end{bmatrix} = \begin{bmatrix} \cos \theta & \sin \theta & 0 \\ -\sin \theta & \cos \theta & 0 \\ 0 & 0 & 1 \end{bmatrix} \begin{bmatrix} x_r - x \\ y_r - y \\ \theta_r - \theta \end{bmatrix}\quad (19)$$

Therefore, it is obtained the tracking error

$$\begin{aligned}\dot{x}_e &= \omega y_e - v + v_r \cos \theta_e \\ \dot{y}_e &= -\omega x_e + v_r \sin \theta_e \\ \dot{\theta}_e &= \omega_r - \omega\end{aligned}\quad (20)$$

For convenience, new coordinates and inputs (Murray *et al.*, 1993) are chosen:

$$\begin{bmatrix} x_0 \\ x_1 \\ x_2 \end{bmatrix} = \begin{bmatrix} \theta_e \\ y_e \\ -x_e \end{bmatrix}, \quad \begin{bmatrix} u_0 \\ u_1 \end{bmatrix} = \begin{bmatrix} \omega_r - \omega \\ v - v_r \cos x_0 \end{bmatrix}\quad (21)$$

Equation (20) can be rewritten as

$$\begin{aligned}\dot{x}_0 &= u_0 \\ \dot{x}_1 &= (\omega_r - u_0)x_2 + v_r \sin x_0 \\ \dot{x}_2 &= -(\omega_r - u_0)x_1 + u_1\end{aligned}\quad (22)$$

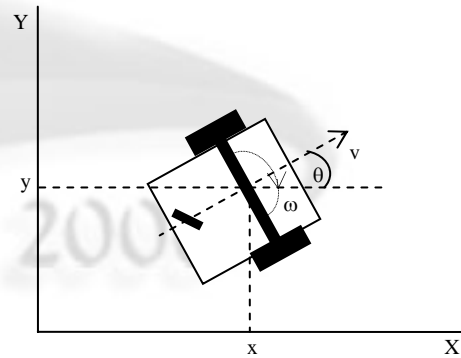


Fig. 7. Geometric description of the mobile robot.

With the new coordinates (x_0, x_1, x_2) , the tracking problem is transformed now into a regulation problem. The transformation above is invertible, and $(x_0, x_1, x_2) = (0, 0, 0)$ is equivalent to $x = x_r, y = y_r, \theta = \theta_r$. Therefore, by inverse transformation of coordinates, if (x_0, x_1, x_2) converges to zero, then the tracking problem is solved.

Let us consider the linearized model of (20), at the equilibrium point $(0, 0, 0)$.

$$\dot{\tilde{x}} = \begin{bmatrix} 0 & 0 & 0 \\ v_r & 0 & \omega_r \\ 0 & -\omega_r & 0 \end{bmatrix} \tilde{x} + \begin{bmatrix} 1 & 0 \\ 0 & 0 \\ 0 & 1 \end{bmatrix} \begin{bmatrix} \bar{u}_0 \\ \bar{u}_1 \end{bmatrix}\quad (23)$$

It can be noted that this linearized model is stabilizable by using a feedback linear control for the case $v_r^2(t) + \omega_r^2(t) \geq \varepsilon > 0$, for all $t \geq 0$.

4.1 H_∞ Control

The linearized model (23) for the case of the H_∞ controller design can be rewritten as:

$$\begin{aligned}\dot{\bar{x}} &= A\bar{x} + B\bar{u} + B_w w \\ z &= Cx\end{aligned}\quad (24)$$

where $A = \begin{bmatrix} 0 & 0 & 0 \\ v_r & 0 & \omega_r \\ 0 & -\omega_r & 0 \end{bmatrix}$; $B = \begin{bmatrix} 1 & 0 \\ 0 & 0 \\ 0 & 1 \end{bmatrix}$; w represents

the non-modeled perturbations; $B_w = [1 \ 0 \ 1]^T$ and

$$C = \begin{bmatrix} 1 & 0 & 0 \\ 0 & 1 & 0 \\ 0 & 0 & 1 \end{bmatrix}.$$

The sampling time of the Pioneer 2DX mobile robot is $T_s=0.1$ sec, then, the model (24) should be discretized with this sampling time. By resorting to Euler discretization, the discrete model can be attained

$$\begin{aligned}\bar{x}_{k+1} &= A_d \bar{x}_k + B_d \bar{u}_k + B_{wd} w_k \\ z_k &= C \bar{x}_k\end{aligned}\quad (25)$$

where $A_d=(I+T_s A)$, $B_d=T_s B$ and $B_{wd}=T_s B_w$. To obtain the controller, the next problem is considered.

Let \bar{x}_k be the state of the system (24). Then, the feedback state matrix gain K within the control law $\bar{u}_k = K \bar{x}_k$ is given by $K = YQ^{-1}$, where $Q > 0$ and Y are obtained from the solution (if it exists) of the following minimization problem with a linear objective:

$$\begin{aligned}\min_{\gamma, Q, Y} & \gamma \\ \text{Subject to} & \\ & Q > 0\end{aligned}\quad (26)$$

$$\begin{bmatrix} Q & A_d Q + B_d Y & C_d Q \\ Q A_d^T + Y^T B_d & Q + B_{wd}^T \gamma^{-1} B_{wd} & 0 \\ Q C_d^T & 0 & I \end{bmatrix} \leq 0$$

Brief technical explanation (Boyd *et al.*, 1994): Choosing the following Lyapunov candidate function

$$V = x_k^T P x_k$$

it should satisfy

$$\Delta V \leq \gamma^2 w_k^T w_k - z_k^T z_k$$

Solving this last inequality, (26) is obtained, where $P = Q^{-1}$.

The equation for the linear trajectory along the corridor is

$$\begin{aligned}x_r &= 0 \\ y_r &= 0.2t \\ \theta_r &= 0 \\ v_r &= \sqrt{\dot{x}_r^2 + \dot{y}_r^2} = 0.2 \\ \omega_r &= 0\end{aligned}$$

For the system (26) a H_∞ controller is obtained using the Matlab LMI Control Toolbox (Gahinet *et al.*, 1994). The feedback gain is,

$$K = \begin{bmatrix} -2.4808 & -2.3184 & 0.0001 \\ -0.0002 & -0.0003 & -2.2047 \end{bmatrix}.$$

5 Experimental Results

In order to evaluate the performance of the proposed control system, several experiences were done on a Pioneer 2DX mobile robot with an on-board Sony PTZ CCD camera (Fig. 8).



Fig. 8 The mobile robot Pioneer 2DX.

The corridor perspective lines are calculated using Hough transform. The information of the image processing is updated every 200 msec. The camera constants values are: $\alpha_x=166000$ $\alpha_y=166000$ pixels/m, $\lambda=0.0054$ m, $\gamma=-5^\circ$, $h=0.31$ m. The robot navigates with linear velocity $v=0.2$ m/s. The Fig. 9 shows the trajectory of the robot navigating along a corridor at the Institute of Automatics, National University of San Juan, Argentina. The experiment is designed in a way that the robot finds different sensing and environment conditions during navigation. The data fusion obtained from ultrasonic sensors and perspective lines is shown in Fig. 10. Fig. 11 depicts the control action obtained from the controller; the resolution is 1deg/s. The experiment shows a good performance of the robot evolution when navigating along the corridor centerline, independently of the varying environment conditions.

6 Conclusions

This work has presented a control strategy for mobile robots navigating in corridors, using the fusion of data signals from vision and ultrasonic sensors. The

controllers generate angular velocity commands to keep the robot navigating along the corridor with constant linear velocity. The fusion of both data signals was realized by using a distributed information filter; DIF. Experiments on a laboratory robot were presented, showing the performance of the proposed control system.

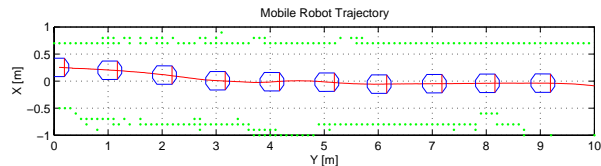


Fig. 9. Mobile robot trajectory.

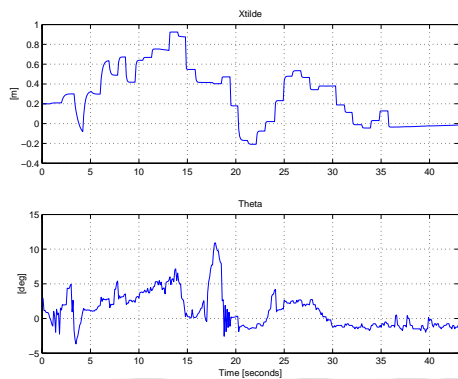


Fig. 10. X-tilde and Theta from data fusion.

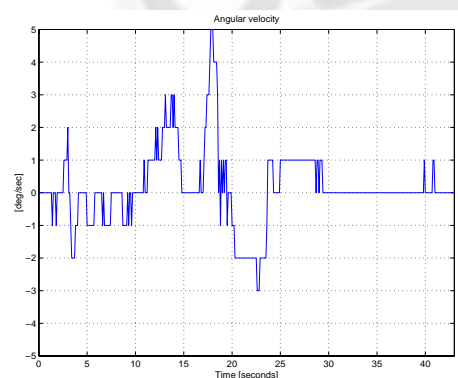


Fig. 11. Control action

7 Acknowledgements

The authors gratefully acknowledge SETCIP and CONICET (Argentina), and the *Universidade Federal de Sergipe* (Brazil) for partially funding this research.

References

Bemporad, M., Di Marco and A. Tesi. (1997). Wall-following controllers for sonar-based mobile robots. *Proc. 36th. IEEE Conf. on Decision and Control*, San Diego.

Bicho, E. (1999). The dynamic approach to behavior-based robotics. *PhD. Thesis, University of Minho, Portugal*.

Boyd S., L. El Ghaoui, E. Feron and V. Balakrishnan, (1994). *Linear Matrix Inequalities in Systems and Control Theory*, Philadelphia, PA: SIAM.

Carelli, R., C. Soria, O. Nasisi and E. Freire. (2002). Stable AGV Corridor Navigation with Fused Vision-Based Control Signals. *In: IECON'02 – 28th Annual Conference of the IEEE Industrial Electronics Society*, Sevilla. pp. 2433-2438.

Dev, A., B. Kröse and F. Groen. (1997). Navigation of a mobile robot on the temporal development of the optic flow. *Proc. Of the IEEE/RSJ/GI Int. Conf. On Intelligent Robots and Systems IROS'97*, Grenoble, pp. 558-563.

Dixon, W., D. Dawson, E. Zergeroglu and A Behal. (2001). Nonlinear Control of wheeled mobile robots. *Springer Verlag*.

Freire, E., T. Bastos Filho, M. Sarcinelli Filho and R. Carelli. (2004). A New Mobile Robot Control Architecture: Fusion of the Output of Distinct Controllers. *IEEE Transactions on Systems Man and Cybernetics Part B-Cybernetics*, v. 34, n. 1, p. 419-429.

Gahinet P, N. Arkadii *et al.* (1994). “The LMI Control Toolbox”, *Proc. of 33rd Conf. On Decision and Control*, Lake Buena Vista, Florida, pp. 2038-2041.

Mattei M. (2000). Sufficient conditions for the synthesis of H_{∞} fixed-order controllers. *International Journal of Robust and Nonlinear Control*, 10, 1237-1248.

Nesterov Y. and A. Nemirovski, (1996). “An interior-point method for generalized linear-fractional problems”, *Math. Programming Ser. B*.

Saeki M. and Aimoto K., (2000). PID controller optimization for H_{∞} control by linear programming. *International Journal of Robust and Nonlinear Control*. 10, 83-99.

Santos-Victor, J., G. Sandini, F. Curotto and S. Garibaldi. (1995). Divergent stereo in autonomous navigation: from bees to robots. *Int. Journal of Computers Vision*, 14-159-177.

Sasiadek, J. Z., P. Hartana. (2000). Odometry and sonar data fusion for mobile robot navigation. 6th IFAC Symposium on Robot Control, SYROCO'00. Vienna, Austria. Preprints, Vol.II, pp.531-536.

Servic, S. and S. Ribaric. (2001). Determining the Absolute Orientation in a Corridor using Projective Geometry and Active Vision. *IEEE Trans. on Industrial Electronics*, vol. 48, No. 3.

Vassallo, R., H. J. Schneebeli and J. Santos-Victor. (1998). Visual navigation: combining visual servoing and appearance based methods. *SIRS'98, Int. Symp. on Intelligent Robotic Systems, Edinburgh, Scotland*.

Yang, Z. and W. Tsai. (1999). Viewing corridors as right parallelepipeds for vision-based vehicle localization. *IEEE Trans. on Industrial Electronics*, vol. 46, No. 3.

Zhou, K., Doyle J. C. and Glover K., (1996). *Robust and Optimal Control*. London: Prentice Hall.